The EMBO Journal Vol.17 No.21 pp.6412–6425, 1998

Distinct roles of two separable *in vitro* activities of yeast Mre11 in mitotic and meiotic recombination

Munenori Furuse[1,2], Yuko Nagase[1,3], Hideo Tsubouchi[4], Kimiko Murakami-Murofushi[3], Takehiko Shibata[1,2] and Kunihiro Ohta[1,5]

[1]Cellular and Molecular Biology Laboratory, The Institute of Physical and Chemical Research (RIKEN), Wako-shi, Saitama 351-0198, [2]The Graduate School of Science and Engineering, Saitama University, Urawa-shi, Saitama 338-8570, [3]Faculty of Science, Ochanomizu University, Bunkyo-ku, Tokyo 112-8610 and [4]Department of Biology, Osaka University, Toyonaka, Osaka 560, Japan

[5]Corresponding author
e-mail: kohta@postman.riken.go.jp

In *Saccharomyces cerevisiae*, Mre11 protein is involved in both double-strand DNA break (DSB) repair and meiotic DSB formation. Here, we report the correlation of nuclease and DNA-binding activities of Mre11 with its functions in DNA repair and meiotic DSB formation. Purified Mre11 bound to DNA efficiently and was shown to have Mn^{2+}-dependent nuclease activities. A point mutation in the N-terminal phosphoesterase motif (Mre11D16A) resulted in the abolition of nuclease activities but had no significant effect on DNA binding. The wild-type level of nuclease activity was detected in a C-terminal truncated protein (Mre11ΔC49), although it had reduced DNA-binding activity. Phenotypes of the corresponding mutations were also analyzed. The *mre11D16A* mutation conferred methyl methanesulfonate-sensitivity to mitotic cells and caused the accumulation of unprocessed meiotic DSBs. The *mre11ΔC49* mutant exhibited almost wild-type phenotypes in mitosis. However, in meiosis, no DSB formation could be detected and an aberrant chromatin configuration was observed at DSB sites in the *mre11ΔC49* mutant. These results indicate that Mre11 has two separable functional domains: the N-terminal nuclease domain required for DSB repair, and the C-terminal dsDNA-binding domain essential to its meiotic functions such as chromatin modification and DSB formation.

Keywords: DNA binding/double-strand break repair/DSB formation/Mre11/nuclease

Introduction

Double-strand DNA lesions caused by factors such as alkylating agents, ionizing radiation, active oxygen radicals and abortive DNA replication, or arising from meiotically induced double-strand DNA breaks (DSBs) at recombination hot spots, are repaired by DSB-repair pathways. In the yeast *Saccharomyces cerevisiae*, there are at least three major pathways for DSB repair. The first two are homologous recombination between homologous sequences (Shinohara and Ogawa, 1995) and non-homologous end-joining (NHEJ) (Boulton and Jackson, 1996; Tsukamoto and Ikeda, 1998) which is a direct ligation of DSB ends. DNA sequences are usually preserved after repair by homologous recombination (accurate repair). In contrast, the other single-strand annealing pathway (Kramer *et al*., 1994; Mezard and Nicolas, 1994; Haber, 1995; Boulton and Jackson, 1996) is accompanied by a deletion in DNA sequence (error-prone repair).

Mre11, Rad50 and Xrs2 proteins in yeast are assumed to play central roles in the homologous recombination and NHEJ pathways probably as a multiple protein complex (Johzuka and Ogawa, 1995; Ogawa *et al*., 1995). This is consistent with the results that the phenotypes of disruption in each gene are indistinguishable from each other, and there is no synergistic effect in double null mutations. Null mutations of these three genes confer hypersensitivity to methyl methanesulfonate (MMS) and ionizing radiation (Game and Motimer, 1974; Farnet *et al*., 1988; Ivanov *et al*., 1992; Johzuka and Ogawa, 1995). Disruption of these genes results in deficiency in NHEJ or illegitimate recombination in mitosis (Milne *et al*., 1996; Moore and Haber, 1996; Tsukamoto *et al*., 1996; Boulton and Jackson, 1998), and exhibits deficiency in meiotic homologous recombination and meiotic DSB formation at recombination hot spots (Cao *et al*., 1990; Ivanov *et al*., 1992; Johzuka and Ogawa, 1995). In addition, meiotic DSBs are not repaired properly in a subset of separation-of-function mutations in *RAD50* (*rad50S*) (Cao *et al*., 1990) and *MRE11* (*mre11S*) (Nairz and Klein, 1997; Tsubouchi and Ogawa, 1998), in which unprocessed DSBs are accumulated during meiosis. In such mutants, a type II topoisomerase-like factor Spo11 (Bergerat *et al*., 1997; Keeney *et al*., 1997) is left attached covalently to the 5′ termini of the DSBs (Keeney *et al*., 1997), thereby no resection occurs at ends of the DSBs.

Mre11 and Rad50 are highly conserved proteins also found in *Schizosaccharomyces pombe* (Tavassoli *et al*., 1995), mouse and human cells (Petrini *et al*., 1995). Recently, a functional homologue of *XRS2* in human cells turned out to be a gene responsible for Nijmegen breakage syndrome which is a variant of ataxia telangiectasia characterized by ionizing radiation sensitivity, immunodeficiency and an increased incidence of cancer (Carney *et al*., 1998; Matsuura *et al*., 1998; Varon *et al*., 1998). In human cells, Mre11, Rad50 and Xrs2 proteins were shown to form a complex as observed in yeast cells (Dolganov *et al*., 1996; Carney *et al*., 1998). These data suggest that the DSB-repair system of Mre11–Rad50–Xrs2 is a key element of eukaryotic DSB repair which is highly conserved in all eukaryotes.

Mre11–Rad50–Xrs2 proteins play other important roles in maintenance and stability of chromosomes. Yeast Mre11 and Rad50 proteins are required for telomere maintenance

(Kironmai and Muniyappa, 1997; Boulton and Jackson, 1998; Nugent *et al*., 1998), homologous pairing (Loidl *et al*., 1994; Weiner and Kleckner, 1994), and suppression of mitotic interchromosomal recombination (Farnet *et al*., 1988; Alani *et al*., 1990; Ajimura *et al*., 1993; Johzuka and Ogawa, 1995). In addition, mutations in these genes confer an aberrant level of hypersensitivity to micrococcal nuclease (MNase) at DSB sites in premeiosis and meiosis (Ohta *et al*., 1998). DSB sites in *S.cerevisiae* exhibit hypersensitivity to DNase I (Wu and Lichten, 1994; Fan and Petes, 1996; Keeney and Kleckner, 1996) and MNase (Ohta *et al*., 1994). MNase hypersensitivity at DSB sites in *ARG4* and *CYS3* loci increases during meiosis prior to DSB formation (Ohta *et al*., 1994). Analysis of the chromatin configuration at DSB sites in *mre11, rad50* and *xrs2* mutants revealed that MNase hypersensitivity at DSB sites in *mre11* mutant stays at the premeiotic level, while the other two mutants exhibit increases in MNase hypersensitivity comparable to that in wild-type cells (Ohta *et al*., 1998). In addition, *mre11* mutation is epistatic to *rad50* with respect to the effects in chromatin configuration at DSB sites, suggesting that Mre11 protein plays a more fundamental role at DSB sites in chromatin.

Mre11 protein has a homology to *Escherichia coli* SbcD nuclease which forms a complex with SbcC, an *E.coli* counterpart of Rad50 proteins (Leach *et al*., 1992; Sharples and Leach, 1995; Connelly and Leach, 1996). SbcD and Mre11 share a consensus motif for various phosphoesterases in the N-terminal domain (Sharples and Leach, 1995). On the other hand, SbcD lacks the clusters of charged amino acids in the C-terminal domain of Mre11. Therefore, Mre11 seems to consist of at least two domains: an N-terminal nuclease domain homologous to SbcD, and a C-terminal eukaryote-specific domain with charged amino acids clusters.

To examine the role of the Mre11 protein, we have studied the relationship between *in vitro* biochemical properties and *in vivo* functions, using yeast Mre11 proteins along with two mutant proteins having a mutation on either N-terminal or C-terminal domains. The present results indicate that Mre11 consists of two separable functional domains: the N-terminal domain which is essential to the nuclease activity of Mre11 *in vitro* and recombination repair *in vivo*, and the C-terminal domain which is important for dsDNA-binding activity of Mre11 *in vitro* and essential for *in vivo* meiotic functions such as meiotic DSB formation, meiotic recombination and meiotic changes in chromatin configuration at DSB sites.

Results

DNA-binding activity of the Mre11 protein: a role for the C-terminal domain

To study biochemical properties of Mre11 protein, we generated three constructs for expression in *E.coli* including wild-type and two mutants: an N-terminal phosphoesterase mutation and a C-terminal truncated protein (Figure 1). In the N-terminal mutation, we introduced an amino acid substitution at Asp16 to Ala (Mre11D16A) (Figure 1). This residue is well conserved in all known Mre11 proteins and various phosphoesterases (Figure 1). From the analysis of X-ray diffraction studies, this residue was shown to be in the active center and important for the binding of the Fe^{3+} ion in a phosphoesterase calcineurin A (Griffith *et al*., 1995; Kissinger *et al*., 1995). Site-directed mutagenesis at the corresponding Asp in bacteriophage λ phosphoprotein phosphatase (Figure 1) resulted in a 10^6-fold reduction in K_{cat} (Zhuo *et al*., 1994). The C-terminal truncation mutant (Mre11ΔC49) lacks 49 amino acids in the C-terminus of Mre11. This region consists of a cluster of basic amino acids which is absent in *E.coli* SbcD protein (Figure 1).

All types of proteins were expressed in *E.coli*, and the cell extracts were fractionated through a Co^{2+} chelating affinity column, since they have a $(His)_6$-tag in the N-termini. We confirmed that tagging in the N-terminus does not prevent *in vivo* functions of Mre11 (data not shown). TALON-purified fractions were further purified through a heparin–Sepharose or a dsDNA–cellulose column. All proteins bound to the heparin–Sepharose column efficiently. The wild-type Mre11 and Mre11D16A proteins could bind to a dsDNA–cellulose column (Figure 2A and B). They were eluted from dsDNA–cellulose at a moderately high concentration of salt (400–500 mM NaCl). Mre11ΔC49 did not bind to dsDNA–cellulose efficiently, but could be fractionated through heparin–Sepharose and Q–Sepharose columns. The fraction purified by heparin–Sepharose or dsDNA–cellulose was further fractionated through phenyl–Sepharose chromatography. The purity of the Mre11 proteins after the heparin or DNA–cellulose chromatography was nearly homogeneous (Figure 2B).

We studied Mre11 proteins further using gel-filtration column chromatography to examine their apparent molecular weights. All Mre11 proteins eluted between catalase (mol. wt: 230 000) and aldolase (mol. wt: 158 000) (Figure 2C). Estimated molecular weights of Mre11 proteins are ~200 000, which is slightly higher than twice the molecular weight for monomeric $(His)_6$-tagged Mre11 proteins that has been deduced from amino acid sequences [wild-type $(His)_6$-Mre11: 82 112, $(His)_6$-Mre11D16A: 82 068, $(His)_6$-Mre11ΔC49: 76 819]. These results suggest that Mre11 protein can exist in a multimeric form as human Mre11 protein (Paull and Gellert, 1998). We could not detect any significant difference in the apparent molecular weights of wild-type Mre11, Mre11D16A and Mre11ΔC49 proteins, indicating that none of the mutations affected overall protein configuration.

Using purified Mre11 proteins, we first examined DNA-binding activities using a band-shift assay. A linearized pUC118 DNA substrate was mixed with the purified wild-type Mre11 in the presence of Mg^{2+}. Protein–DNA complexes were analyzed by non-denaturing agarose gel electrophoresis followed by staining with ethidium bromide (Figure 3A). In the presence of Mre11, we detected a mobility shift of a dsDNA band. Binding of Mre11 to dsDNA does not need free DNA ends, since we detected similar mobility shifts using a supercoiled dsDNA substrate (data not shown). We could not find strict sequence specificity in DNA binding of Mre11.

To study further DNA-binding specificity of Mre11, various types of ss- or ds- ^{32}P-labeled or non-labeled oligonucleotide substrates (Figure 3F) were mixed with Mre11 in the presence of Mg^{2+}, and the resulting complex was analyzed by non-denaturing polyacrylamide gel electrophoresis followed by analysis with a radioactivity

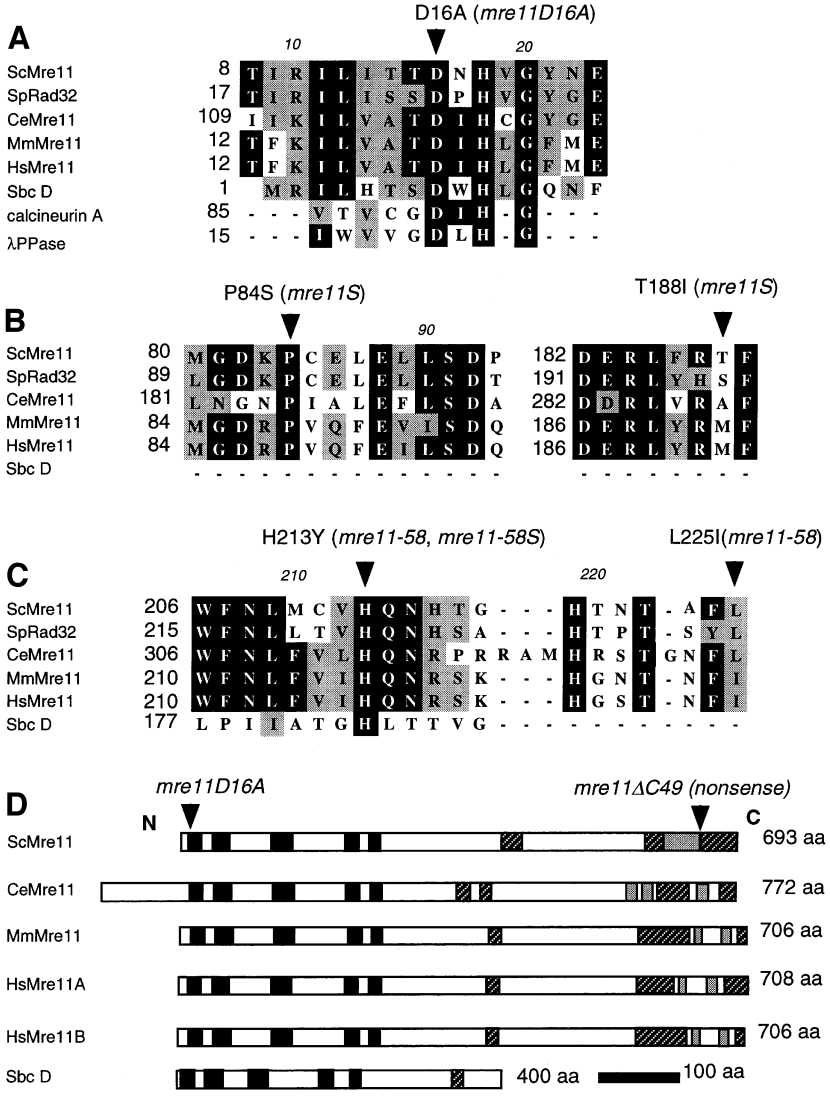

Fig. 1. Sites of *mre11* mutations. (**A**–**C**) Amino acid sequences around *mre11D16A*, *mre11S*, *mre11-58* and *mre11-58S* mutations in *MRE11* and other related phosphoesterases. Residues indicated with dark or light shadings represent identical or similar amino acids, respectively. Arrowheads show the positions of the mutations indicated. Numbers represent positions of amino acids from the first methionine. ScMre11, *S.cerevisiae* Mre11 (Johzuka and Ogawa, 1995); SpRad32, *S.pombe* Rad32 (Tavassoli *et al*., 1995); CeMre11, *Caenorhabditis elegans* Mre11 (DDBJ/EMBL/GenBank accession No. Z73978); MmMre11, *Mus musculus* (DDBJ/EMBL/GenBank accession No. U58987); HsMre11, *Homo sapiens* (Petrini *et al*., 1995; Paull and Gellert, 1998); SbcD (Leach *et al*., 1992); calcineurin A (Guerini and Klee, 1989); λPPase (Cohen *et al*., 1988). (**D**) Positions of *mre11D16A* and *mre11ΔC49* mutations in a schematic drawing of Mre11 protein. Domain structures of other Mre11 and SbcD proteins are also indicated. HsMre11A is from Petrini *et al*. (1995) and HsMre11B from Paull and Gellert (1998). Black boxes indicate motifs for metal-phosphoesterases. Hatched and shaded boxes represent basic and acidic amino acid clusters.

image analyzer or with a fluorescence image analyzer after staining with ethidium bromide. It was shown that binding to ds-oligonucleotides (30mer) is more efficient than that to ss-oligonucleotides (30mer) (Figure 3B and D). However, Mre11 bound to oligonucleotides less efficiently compared with longer DNA substrates such as plasmid DNA. In fact, the efficiency of the binding was dependent upon the length of the duplex in the oligonucleotides rather than the structure of DNA substrates (Figure 3C and E). Binding of Mre11 to DNA substrates with 3′-overhangs seemed to be slightly stronger than that to substrates with the corresponding length of 5′-overhangs (~2.2-fold in the case of 7 nt overhangs). We also detected a 1.8- to 2.5-fold enhancement in the binding of Mre11 to ds-oligonucleotide substrates (28mer) with cohesive 4 nt overhangs, compared with a substrate with non-cohesive overhangs of a similar length (Figure 3C and E), suggesting that annealing and catemer formation at the complementary ssDNA overhangs facilitates the binding of Mre11 to DNA.

We found that Mre11 protein has a transitional metal-dependent dsDNA-binding activity. In a condition where limited amount of Mre11 exists, Mre11 weakly bound to dsDNA regardless of the presence or absence of Mg^{2+} (Figure 4B). On the other hand, in such a condition, transition metal divalent cations (e.g. Mn^{2+}, Zn^{2+}, Cu^{2+}, Ni^{2+}) enhanced the binding of Mre11 to dsDNA substrates (Figure 4B). This may not be simply due to the $(His)_6$-tag in the N-terminus of the Mre11 protein, since other DNA-binding proteins [HisMts1, a CREB-type transcrip-

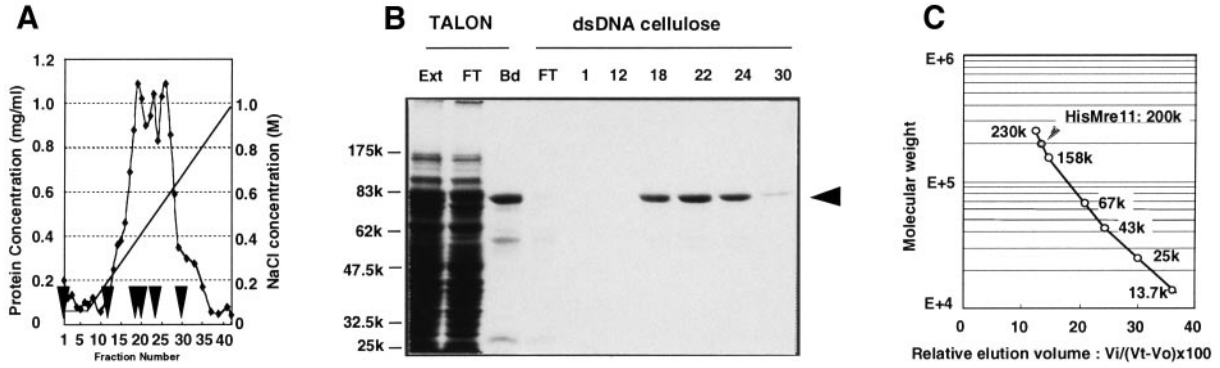

Fig. 2. Fractionation of wild-type and mutant Mre11 proteins. (**A**) The protein elution profile of a DNA affinity chromatography of the wild-type $(His)_6$-Mre11 protein. $(His)_6$-Mre11 proteins were expressed in *E.coli*, and the cell extracts were applied to a TALON cobalt^{2+}-affinity column (Clontech). The TALON-purified fraction was then fractionated through dsDNA–cellulose column. (**B**) Fractions indicated by arrowheads in (A) were analyzed by a 7.5% SDS–PAGE. TALON-purified fraction includes proteolytic fragments of Mre11 proteins, but the purity of the fractions after dsDNA–cellulose is nearly homogenous. Molecular weight markers are maltose-binding protein-β-galactosidase, 175 000; maltose-binding protein-paramyosin, 83 000; glutamic dehydrogenase, 62 000; aldolase, 47 500; and triosephosphate isomerase, 32 500. The lanes Ext, FT, and Bd in the TALON chromatography represent *E.coli* extracts, flow-through and bound fractions, respectively. The lane FT in dsDNA–cellulose chromatography indicate the flow-through fraction. The numbers for each lane indicates the fraction number. (**C**) Gel purification of Mre11 proteins. Mre11 proteins were fractionated through Superose 12HR as described in Materials and methods. All Mre11 proteins (wild-type, D16A, ΔC49) eluted between catalase and aldolase. Molecular weight standards are catalase (230 000), aldolase (158 000), BSA (67 000), ovalbumin (43 000), chymotrypsin (25 000), RNase A (13 700) and tryptophan (186). The arrowhead indicates the positions of Mre11.

tion factor in *S.pombe* (Kon *et al.*, 1997)] with an N-terminal $(His)_6$ did not show such a transitional metal-dependent enhancement (Figure 4C).

DNA-binding activities of mutant Mre11 proteins were examined by band-shift analysis using plasmid dsDNA (Figure 4C). Mre11D16A exhibited almost the same level of DNA band-shift activity in the wild-type Mre11. On the other hand, Mre11ΔC49 protein showed only a weak band shift even in the presence of transition divalent cations. This is consistent with the results of DNA–cellulose affinity chromatography (see above). These results can be rationalized by a loss of cooperativity in Mre11ΔC49 protein. However, the reduction in the DNA-binding activity of Mre11ΔC49 protein was also observed when we used oligonucleotide substrates (30mer) in which less cooperative binding could be expected (data not shown). From these results, we concluded that C-terminal domain is important for the DNA-binding activity of Mre11 protein.

N-terminal phosphoesterase domain is involved in nuclease activity of Mre11

Extensive homology in the N-terminal domain of Mre11 to *E.coli* SbcD nuclease suggests that Mre11 has a nuclease activity. In fact, human Mre11 protein exhibits exo- and endo-nuclease activities (Paull and Gellert, 1998; Trujillo *et al.*, 1998). To examine nuclease activity of yeast Mre11, *E.coli*-expressed $(His)_6$-Mre11 was incubated with a circular M13 viral ssDNA substrate in the presence of Mn^{2+} (Figure 5A). Mre11 cleaved circular M13 ssDNA in the presence of Mn^{2+} (0.5–10 mM), but we could not detect significant nuclease activity in the absence of Mn^{2+} or in the presence of other divalent cations (Mg^{2+}, Ni^{2+}, Ca^{2+}, Sr^{2+}, Co^{2+} and Zn^{2+}). The nuclease activity did not require ATP. A linearized plasmid DNA can be a nuclease substrate of Mre11 in the presence of Mn^{2+} (Figure 5B). Supercoiled or relaxed closed circular dsDNA was not digested by Mre11 (data not shown), indicating that digestion of dsDNA requires the ends of DNA. We detected an exonuclease activity on ds-oligonucleotides with blunt and 5′-overhangs at both ends, but not on ds-oligonucleotides with 3′-overhangs at both ends (Figure 5C). When we incubated Mre11 protein with 5′ ^{32}P-labeled linearized plasmid DNA with 5′-overhangs, smear bands were detected after the incubation (Figure 5D). These suggests that Mre11 has 3′ to 5′ double-strand-specific exonuclease activity as observed in human Mre11 protein (Paull and Gellert, 1998; Trujillo *et al.*, 1998).

We next examined nuclease activity of mutant proteins (Figure 5B). Mre11ΔC49 protein has a nuclease activity comparable to the wild-type Mre11, while it shows reduced DNA binding. On the other hand, we could detect no significant nuclease activity in Mre11D16A protein fraction. These observations show that the C-terminal DNA-binding domain is not responsible for the nuclease activity and the N-terminal phosphoesterase domain is required for the nuclease activity. This indicates that the nuclease activity is an intrinsic property of Mre11 protein and is not due to trace amounts of contaminating proteins.

Phenotypes of mre11D16A and mre11ΔC49 mutations during mitosis

To study the relationship between the *in vitro* properties of Mre11 and *in vivo* functions, we introduced the corresponding mutations (*mre11D16A* and *mre11ΔC49*, see Figure 6A) into the yeast genome. We first examined mitotic effects. The mutant *mre11D16A* exhibited strong MMS sensitivity, but it was ~1/10 less sensitive than the case of a null mutant (Figure 6B and C). On the other hand, we could not detect any significant difference in MMS sensitivity of *mre11ΔC49* and the wild-type. In both *mre11D16A* and *mre11ΔC49* strains, we did not detect hyper-recombination (Table I) and slow growth phenotypes that are observed in *mre11* null mutants. In *mre11ΔC49* strain, the interchromosomal recombination rate was reproducibly smaller than the wild-type level (Table I).

Telomere length was also analyzed in these mutants (Figure 7). No detectable difference in the telomere length could be seen between the wild-type and *mre11ΔC49* strains. However, telomere length was shortened in the *mre11D16A*

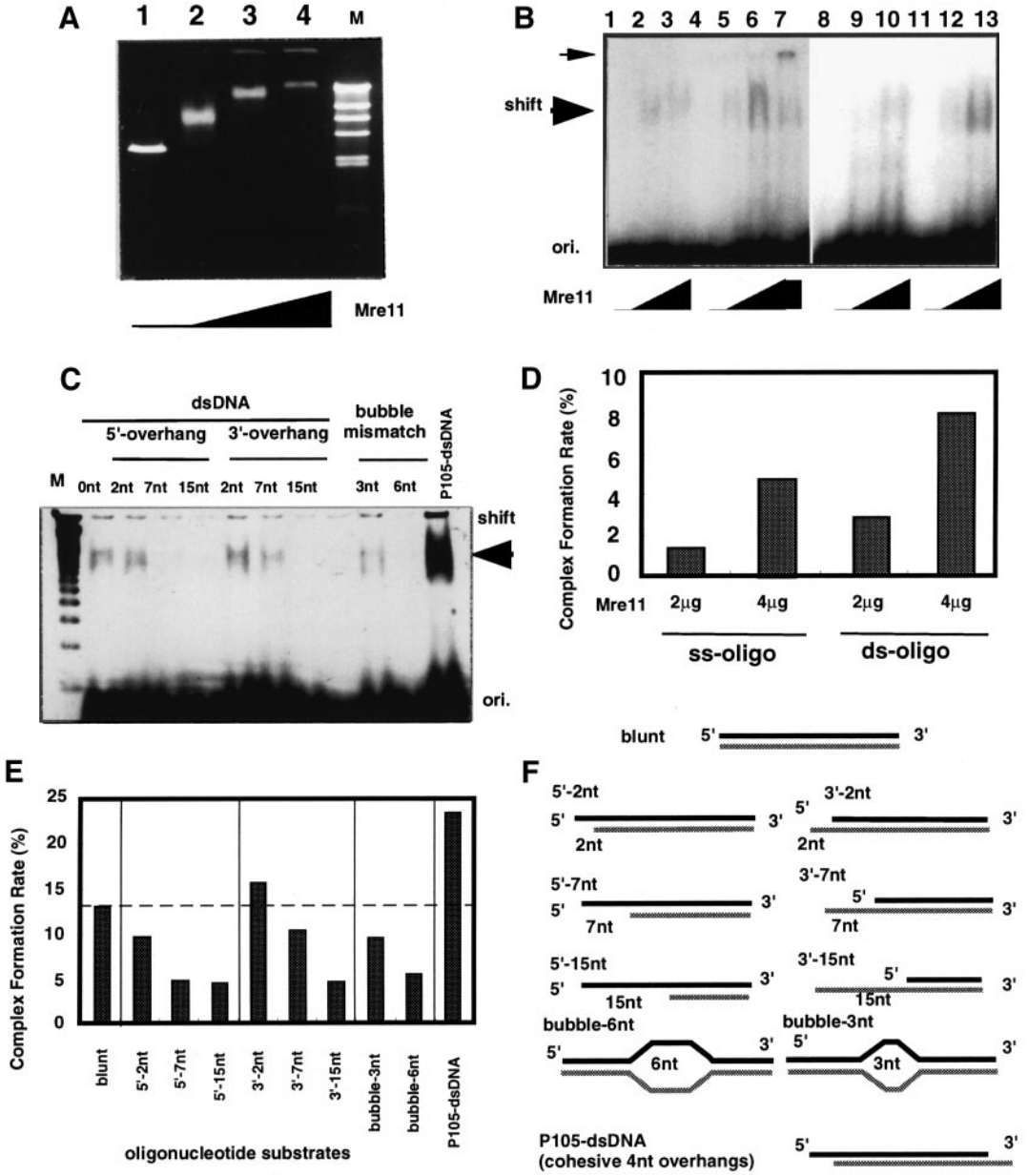

Fig. 3. DNA-binding activity of the wild-type Mre11 protein. (**A**) Binding of Mre11 to linearized pUC118 dsDNA. Heparin-purified wild-type Mre11 protein (lanes 1–4; 0, 1, 2, 4 μg, respectively) was added to 50 ng of *Pst*I-digested pUC118 plasmid DNA. Protein–DNA complexes were then analyzed by a non-denaturing agarose gel (0.8%) electrophoresis followed by staining with ethidium bromide. Lane M represents molecular weight markers (*Hin*dIII digestion of phage λ DNA, 23.1, 9.4, 6.6, 4.3, 2.3, 2.0, 0.56 kb). (**B**) Band-shift analysis using 5′ [^{32}P]end-labeled oligonucleotides. Heparin-purified wild-type Mre11 protein (0 μg in lanes 1, 4, 8, 11; 2 μg in lanes 2, 5, 9, 12; 4 μg in lanes 3, 6, 7, 10, 13) was added to 5 nmol phosphate of non-labeled oligonucleotide substrates [lanes 1–3, poly(dT)$_{14}$ T14; lanes 4–7 and 11–13, ds-oligonucleotide composed of Aarg4 and BantiA; lanes 8–10, ss-oligonucleotide Aarg4, respectively] including 20 fmol of 5′ ^{32}P-labeled molecules. In lane 7, ~1 μg of affinity-purified anti-Mre11ΔC49 protein antibody was added to the reaction mixture for lane 6. In this case, a supershift of DNA–protein complex was observed (small arrow), indicating that the band-shift activity is due to Mre11 protein. Protein–DNA complex was analyzed in 4% non-denaturing PAGE. A large arrow shows the position of the band shift in the presence of Mre11 protein. (**C**) Band-shift analysis using various types of non-labeled ds-oligonucleotides. Six micrograms of purified Mre11 protein was incubated with 5 nmol phosphate of non-labeled oligonucleotide substrates as shown in (F), and analyzed as described in (B). Lane M indicates 100 bp DNA ladders. An arrow indicates the position of the band shift. (**D**–**E**) Quantitative analysis of the band-shift assay [(D) for the panel (B), and (E) for the panel (C)]. In D, lanes 2 (2 μg of Mre11 with ss-oligo), 3 (4 μg of Mre11 with ss-oligo), 5 (2 μg of Mre11 with ds-oligo) and 6 (4 μg of Mre11 with ds-oligo) were analyzed. Band intensities of the shifted bands were measured and % ratio relative to the intensities at the unbound origin were indicated. A dashed line in (E) shows the level of the blunt end ds-oligonucleotide substrate. (**F**) Schematic drawing of oligonucleotides used for the band-shift assay. P105-dsDNA has cohesive complementary 4 nt overhangs at both ends.

strains as observed in the *mre11* and *rad50* null mutant (Kironmai and Muniyappa, 1997; Boulton and Jackson, 1998; Nugent *et al*., 1998). In summary, during mitosis, *mre11D16A* showed deficiency in the repair of DNA damage by MMS and the maintenance of telomere length, but did not exhibit slow growth and hyper-recombination. The mutant *mre11ΔC49* showed almost wild-type phenotypes during mitosis except for a slight hypo-recombination phenotype.

Meiotic phenotypes

Next we examined meiotic phenotypes of these mutants. Frequency of meiotic recombination between *arg4* non-

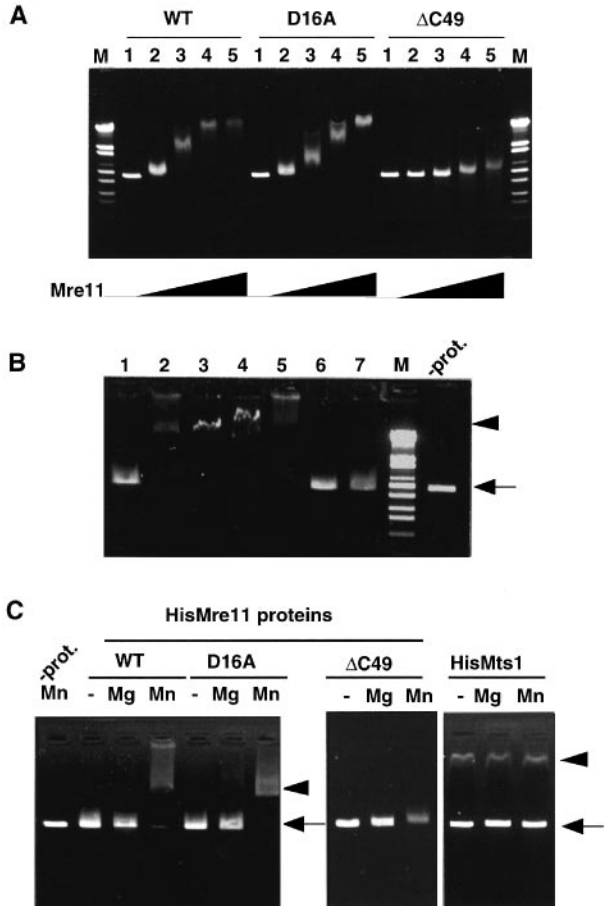

Fig. 4. DNA-binding activity of mutant Mre11 proteins. (**A**) Band-shift activity of mutant Mre11 proteins using a linearized plasmid dsDNA as in Figure 3A. The amount of Mre11 protein used is 0 (lanes 1), 0.5 (lanes 2), 1 (lanes 3), 2 (lanes 4) and 3 μg (lanes 5). Reaction and detection of bands were as described in Figure 3A. Lane M represents molecular weight markers (*Eco*T14I digestion of phage λ DNA, 19.3, 7.7, 6.2, 4.3, 3.5, 2.7, 1.9, 1.5 kb). Note that Mre11ΔC49 protein has less efficient band-shift activity. (**B**) Dependence of the band-shift activity of the wild-type Mre11 protein on metal divalent cations. In this experiment, we used 0.6 μg of Mre11 protein. Lanes 1–7, none, 5 mM of $MgCl_2$, $MnCl_2$, $ZnCl_2$, $CuSO_4$, $NiSO_4$, $SrCl_2$, and $CaCl_2$, respectively. (**C**) Band-shift activity of mutant Mre11 proteins using a linearized plasmid dsDNA in the absence (lanes –) or presence of divalent cations: Mg^{2+} (lanes Mg) or Mn^{2+} (lanes Mn). Lane (–prot.) represents a control without addition of Mre11 proteins. HisMts1 is a $(His)_6$-tagged Atf1/Gad7 transcription factor (Kon *et al*., 1997). In all cases, we used 0.6 μg of proteins. Arrowheads indicate the positions of a supershift. Arrows show the original position of the linearized pUC118 dsDNA.

complementing alleles in the mutants was analyzed by return-to-growth experiments (Figure 8A). In the wild-type, an ~10^3-fold increase in Arg^+ recombinants was detected. However, such a meiotic induction in recombination was completely abolished in the *mre11D16A* and *mre11ΔC49* strains as observed in the null mutant (Figure 8A). Spore formation was reduced to ~50% in the *mre11ΔC49* and null mutants, while the wild-type showed 99% spore formation (Table II). Spore formation in the *mre11D16A* mutant was ~10% even after the incubation for 2 days (Table II). We could find no viable spore in 80 tetrads (320 spores) of the *mre11D16A*, *mre11ΔC49*, and null mutants (Table II).

We then examined meiotic DSB formation at the *YCR48w/YCR47c* meiotic recombination hot spot (Figure 8B). We detected smear DSB bands around the *YCR48w/YCR47c* hot-spot region in the wild-type control at 4–6 h after meiotic induction. On the other hand, no significant signal could be detected in *mre11ΔC49* and null mutants. This is not due to disappearance of Mre11ΔC49 protein in meiotic cells, since Mre11ΔC49 protein can be detected in meiotic cell extracts by immunoblotting with anti-Mre11 protein (data not shown). In the *mre11D16A* mutant, discrete meiotic DSB signals appeared around the hot-spot region at 4 h after meiotic induction, but the DSB was left unprocessed and unrepaired even at 8 h after meiotic induction, as observed in *rad50S* (Cao *et al*., 1990), *mre11S* and *mre11-58* mutants (Nairz and Klein, 1997; Tsubouchi and Ogawa, 1998).

Mre11 is required for the proper meiotic chromatin configuration at DSB sites (Ohta *et al*., 1998). In the wild-type, MNase hypersensitivity at the *ARG4* DSB site increased significantly in meiotic prophase prior to the DSB formation (Ohta *et al*., 1994). However, in *mre11* null mutant, MNase hypersensitivity did not increase during meiosis and stayed at the premeiotic level (Ohta *et al*., 1998). Effects of the *mre11D16A* and *mre11ΔC49* mutations on chromatin configuration were analyzed (Figure 9). MNase-hypersensitivity levels at the *ARG4* DSB site in the *mre11D16A* were very similar to that in the wild-type control both in premeiosis and meiosis (Figure 9A). There was an increase in the hypersensitivity specific to the DSB site during meiosis in the *mre11D16A* mutant as observed in the *rad50S* mutant (Ohta *et al*., 1998). On the other hand, MNase hypersensitivity in *mre11ΔC49* strain did not change significantly during meiosis (Figure 9B). The meiotic hypersensitivity in the *mre11ΔC49* strain stayed at a level very similar to the premeiotic and meiotic level in the *mre11* null mutant (Figure 9C). We confirmed that these effects are specifically found in the DSB site, since little difference in MNase sensitivity was detected at a control sensitive site without meiotic DSB (Figure 9D). In summary, chromatin configuration at the DSB site in *mre11D16A* was indistinguishable from the wild-type and *rad50S*, but that in *mre11ΔC49* was greatly affected in meiosis as observed in the *mre11* null mutant.

Discussion

Mre11 protein consists of two separable functional domains

In this study, we have demonstrated the correlation between the *in vitro* properties of Mre11 protein (nuclease and DNA-binding activities) and *in vivo* functions in DSB repair and meiotic DSB formation using two novel alleles. We also demonstrated that Mre11 can be separated into at least two independent functional domains: the N-terminal SbcD-like nuclease and the eukaryote-specific C-terminal DNA-binding domains. The nuclease domain is involved in some types of DSB repair in mitosis, telomere maintenance and processing of meiotic DSBs. The C-terminal DNA-binding domain is essential for the meiotic functions of Mre11 such as meiotic chromatin modification and DSB formation at recombination hot spots.

The existence of two separable domains in Mre11 was predicted by previous genetic observations of separation-

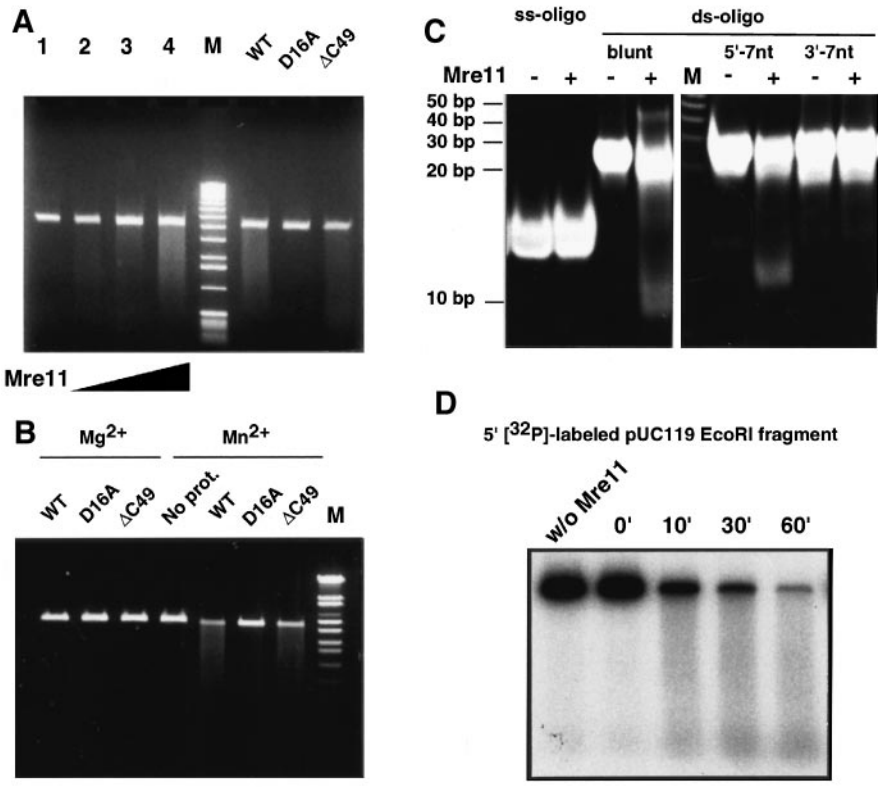

Fig. 5. Nuclease activities of Mre11 proteins. (**A**) Nuclease activity on M13 circular ssDNA. DNA–cellulose-purified wild-type Mre11 protein (lanes 1–4: 0, 1, 2, 4 μg, respectively) was incubated with 200 ng of M13mp18 circular ssDNA at 37°C for 1 h as described in Materials and methods. Digested DNA was analyzed in a 0.8% agarose gel. Lane M indicates 1 kb DNA ladder (Gibco-BRL). Lanes WT, D16A, and ΔC49 show the data using 2 μg of DNA–cellulose-purified wild-type and heparin-purified D16A Mre11 proteins and Q–Sepharose-purified ΔC49 protein, respectively. Note that there is no detectable nuclease activity in Mre11D16A protein. (**B**) Nuclease activity on a linearized plasmid dsDNA. Lanes WT, D16A, and ΔC49 show the data using 1 μg of heparin-purified wild-type and D16A Mre11 proteins and Q–Sepharose-purified ΔC49 protein, respectively. Proteins were incubated with 50 ng of *Eco*RI-digested pUC118 DNA as described in (A). Digested DNA was analyzed on a 0.8% agarose gel. Note that there was no detectable nuclease activity in Mre11D16A protein. Lane M shows molecular size markers of *Eco*T14I-digested phage λ DNA (see Figure 4A). (**C**) Nuclease activity on ds-oligonucleotides. Oligonucleotides Aarg4 and BantiA, K5over7 and BantiA, Aarg4 and L3over7 (see Materials and methods) were annealed to form ds-oligonucleotides with blunt ends (lanes blunt), 7 nt 5′ overhangs (lanes 5′-7nt), and 7 nt 3′ overhangs (lanes 3′-7nt) at both ends, respectively. As described in (A), oligonucleotide substrates including ss-oligonucleotide Aarg4 (2.35 nmol phosphate, 160 pmol DNA ends) were then incubated with 8 μg of wild-type Mre11 protein at 30°C for 1 h. Digested DNA was separated in a 20% polyacrylamide gel and stained with ethidium bromide. Cleavage was only detected in ds-oligonucleotides with blunt ends or 5′ overhangs at both ends. Lane M indicates 10 bp ladders. Numbers indicate base pair numbers of the bands in 10 bp ladders. (**D**) Nuclease activity on *Eco*RI-linearized pUC119 DNA ^{32}P-labeled at the 5′ ends. As described in (A), 5′ ^{32}P-labeled pUC119 plasmid DNA (5 ng) was incubated with 3 μg of wild-type Mre11 protein at 37°C for 0 (lane 0′), 10 (10′), 30 (30′), and 60 min (60′) as described in (A). Bands were detected by autoradiography. Note that smear bands were detected after the incubation.

of-function mutations in *MRE11* (Nairz and Klein, 1997; Tsubouchi and Ogawa, 1998). One type of mutant named *mre11S* and *mre11-58* show a deficiency in DSB repair and processing of meiotic DSBs. Mutations of these alleles are located in different phosphoesterase motifs from the site of the *mre11D16A* mutation. The other type is created by insertions of Ty element in the C-terminal region (Nairz and Klein, 1997). In the latter cases, no DSB can be detected in meiosis. Notably, interallelic complementation occurs in the heterozygous diploids of *mre11S* and C-terminal mutants. Therefore, it is speculated that the mutant proteins may be expressed in the heterozygous cells as partly active configurations and two domains in Mre11 can function independently.

The present results support this idea and give further insight into the domain structure of Mre11 protein. In the present study, we report two new separation-of-function alleles (*mre11D16A* and *mre11ΔC49*) in the N- and C-termini of Mre11 protein. As reported by Nairz and Klein (1997), we observed interallelic complementation in meiotic functions in the heterozygous diploids of *mre11D16A* and *mre11ΔC49* mutations (data not shown). Therefore, it is plausible that the corresponding mutant proteins are partially active in Mre11 activities. We detected nuclease activities in a C-terminal truncated Mre11ΔC49 protein. This means that the rest of Mre11 protein alone can act as a nuclease even in the absence of the C-terminal region. This is consistent with the observation that the homology of Mre11 protein to *E.coli* SbcD nuclease is limited only to the N-terminal portion (about two-thirds of the entire sequence, see Figure 1) which probably includes a DNA-binding site for nuclease activities. The C-terminal region consists of a highly charged domain with acidic and basic amino acid clusters, which are specifically found in Mre11 proteins. In this region, the sequence is not well conserved beyond species, but the clustering of charged amino acids is preserved. We demonstrated that the truncation of the C-terminal

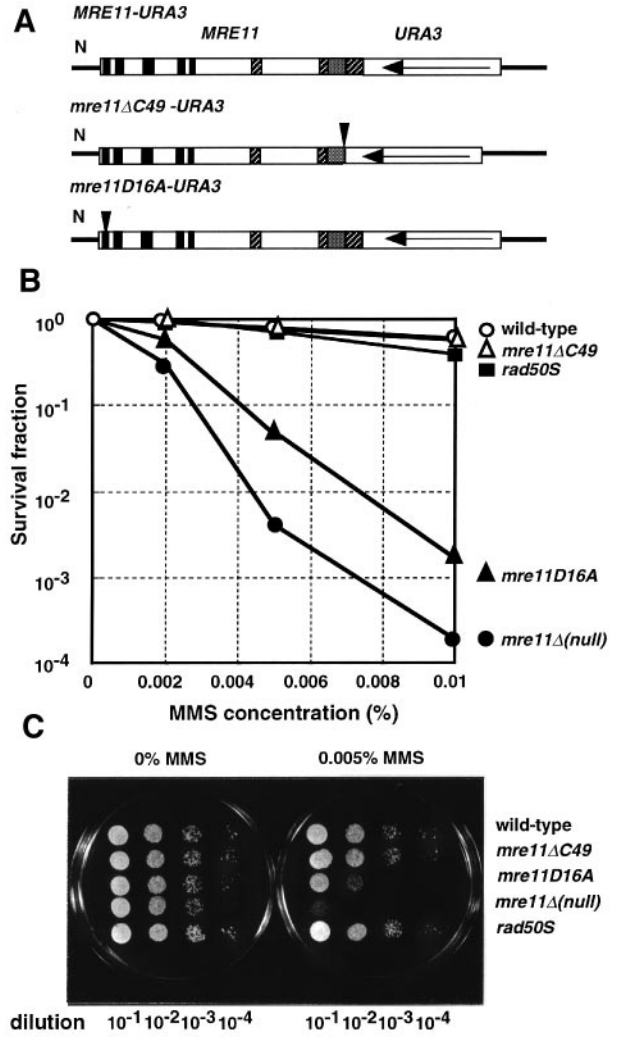

Fig. 6. MMS sensitivity of *mre11D16A* and *mre11ΔC49* mutants. (**A**) Constructions for gene replacement by homologous recombination. All constructs are flanked with *URA3* gene (arrows indicate the direction of transcription) for positive selection of recombinants. Black boxes indicate motifs for metal-phosphoesterases. Hatched and shaded boxes represent basic and acidic amino acid clusters. (**B**) Diploid strains of YMD1599 (a *mre11* null mutant), YMD302 (wild-type), YMD316 (*mre11D16A*), YMD325 (*mre11ΔC49*), and MJL1699 (*rad50S*) were grown in yeast extract, peptone, dextrose (YPD) media, diluted and inoculated on YPD in the presence of the indicated concentration of MMS. Numbers on the plates were counted after incubation for 5 days at 30°C. (**C**) Serial dilution (10^{-1}–10^{-4}) of YPD culture in B (7 μl) was spotted on YPD plates containing 0 or 0.005% of MMS. The plates were incubated for 3 days at 30°C. Strains used are as described in (B).

Table I. Effects of *MRE11* mutations on mitotic interchromosomal recombination

Mutant	Interchromosomal recombination at *arg4-nsp/arg4-bgl* ($\times 10^{-5}$)
Wild-type (YMD302)	5.3 ± 1.4 (n = 3)
mre11Δ-null (YMD1599)	34.6 ± 11.9 (n = 4)
mre11D16A (YMD316)	5.3 ± 1.4 (n = 4)
mre11ΔC49 (YMD325)	1.5 ± 1.0 (n = 4)

Interchromosomal recombination at *arg4-nsp/arg4-bgl* was measured by taking ratios of colony numbers on Arg^- plates to those on Arg^+ plates.

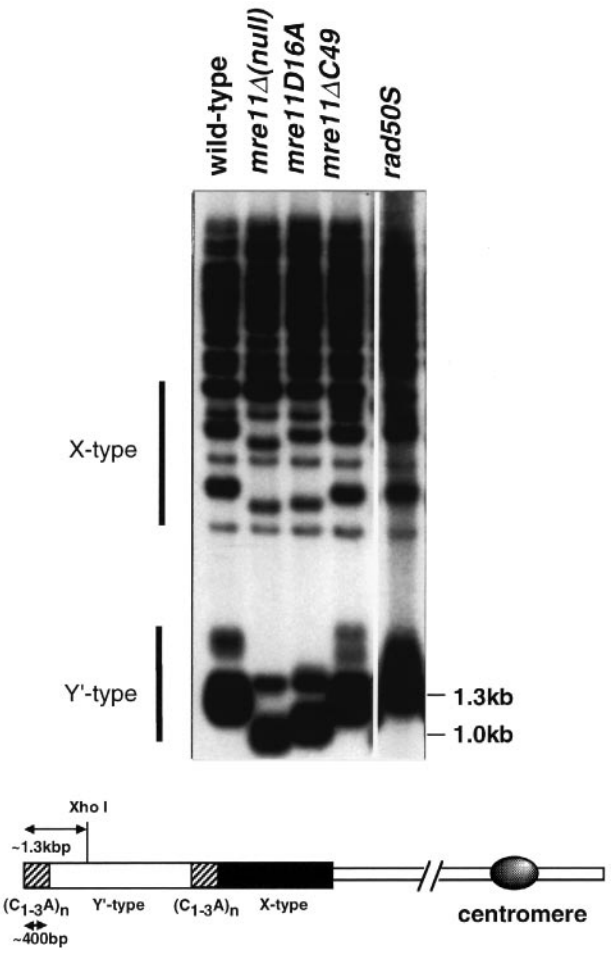

Fig. 7. Telomere length in *mre11D16A* and *mre11ΔC49* mutants. Schematic representation of a yeast chromosome arm indicates the locations of the centromere (indicated by a shaded oval), the telomeric region, the telomeric ($C_{1-3}A$) repeats (hatched boxes), and the X′ (closed box) and Y′ elements (open box). A conserved *Xho*I site is found in the Y′ element. Thus, *Xho*I cleavage of genomic DNA generates ~1.3 kb and larger fragments that can be detected by a poly $(GT)_{20}$ probe. Genomic DNA from diploid strains of YMD1599 (a *mre11* null mutant), YMD302 (wild-type), YMD316 (*mre11D16A*), YMD325 (*mre11ΔC49*) and MJL1699 (*rad50S*) was digested with *Xho*I and separated in 0.8% agarose gel. DNA transferred to a nylon membrane was hybridized with a ^{32}P-labeled poly$(GT)_{20}$ oligonucleotide. Telomeres are shortened in the *mre11D16A* mutant but not in the *mre11ΔC49* strain.

region results in a significant reduction in DNA-binding activity. In addition, the N-terminal phosphoesterase mutant Mre11D16A protein lacks the nuclease activities, but still shows the dsDNA-binding activity comparable to the full-length protein. Thus, the C-terminal region is involved in dsDNA binding which can function independently of the nuclease domain. These results indicate that two domains in Mre11 can function independently.

Multimer formation of Mre11

Results of the gel-filtration analysis of Mre11 proteins suggest that Mre11 protein can exist in a multimeric form. The apparent molecular size of the purified Mre11 was nearly double that of the monomer deduced from its amino acid sequence. In addition, preliminary results of glutaraldehyde crosslinking of Mre11 protein support its existence as a multimers (Y.Nagase, T.Shibata and K.Ohta,

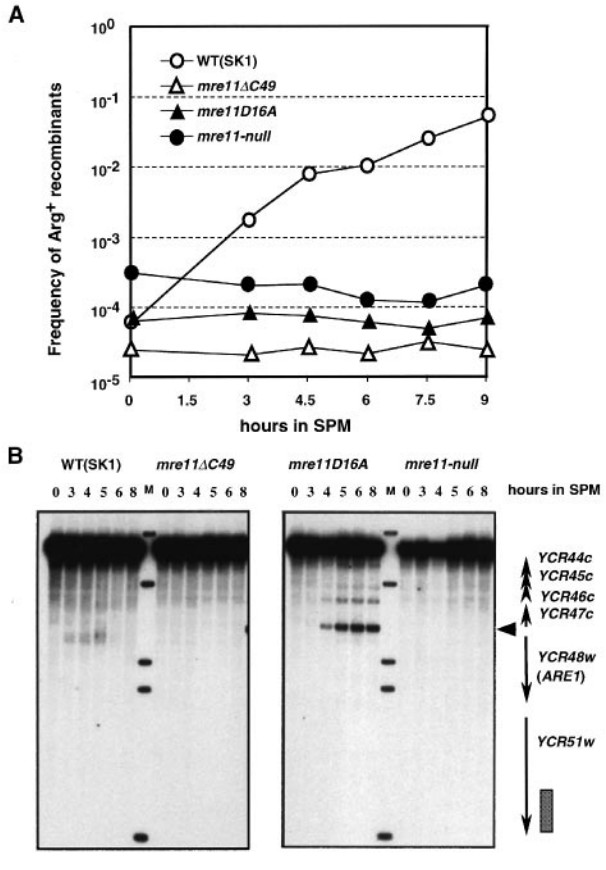

Fig. 8. Deficiency of *mre11D16A* and *mre11ΔC49* mutants in meiotic recombination, DSB formation and its repair. (**A**) Results of return-to-growth experiments. Diploid strains of YMD1599 (a *mre11* null mutant), YMD302 (wild-type), YMD316 (*mre11D16A*), and YMD325 (*mre11ΔC49*) were introduced into meiosis. The horizontal axis represents the time in sporulation medium (SPM). Population of Arg^+ recombinants in *arg4-nsp*/*arg4-bgl* alleles was measured at indicated time points. Each value is the ratio of the number of colonies on Arg^- plates to those on Arg^+ plates. No induction of meiotic recombination can be seen in each *mre11* mutant. (**B**) DSB formation in *mre11* mutants. Genomic DNA from diploid strains of YMD1599 (a *mre11* null mutant), YMD302 (wild-type), YMD316 (*mre11D16A*) and YMD325 (*mre11ΔC49*) was prepared from cells harvested at indicated time points, digested with *Bgl*II, fractionated in a 0.7% agarose gel. DNA transferred to a nylon membrane was hybridized with 0.9 kb *Hin*dIII–*Hin*dIII fragment in *YCR51w* locus. Strong DSB (indicated by an arrow head) at the *YCR47c*/*YCR48w* region can be detected in the wild-type and the *mre11D16A* mutant. Note that no processing and repair of DSB can be detected in the *mre11D16A* mutant. In *mre11ΔC49* and null mutants, no DSB can be detected. Lane M represents molecular size markers (12.4, 6.9, 4.4, 4.0, 0.89 kb, respectively).

unpublished observation). Multimer formation is consistent with previous observations. Two-hybrid analysis using fusion proteins of Gal4–Mre11 and LexA–Mre11 suggested the Mre11–Mre11 interaction in yeast cells (Johzuka and Ogawa, 1995). In addition, interallelic complementation of heterozygotes in *mre11S* and *mre11* C-terminal mutations also suggests the Mre11–Mre11 interaction (Nairz and Klein, 1997). Furthermore, human Mre11 protein is eluted from a gel-filtration column at a position corresponding to ~350 kDa, which is much larger than the estimated monomer molecular size (Paull and Gellert, 1998). The present results of the gel filtration of the Mre11D16A and Mre11ΔC49 proteins suggest that none of the mutations in the phosphoesterase and C-terminal domains affects the multimer formation of Mre11 protein. Thus, a domain for interaction between Mre11 proteins (Mre11–Mre11) should be located in other portions of the molecules.

Roles of the nuclease domain in DNA repair

The novel allele *mre11D16A* exhibits some distinctive phenotypes. The *mre11D16A* mutant shows deficiencies in the repair of DNA damaged by MMS and also in the maintenance of telomere length in mitosis. On the other hand, the *mre11D16A* mutation has no effect on growth rates and interchromosomal recombination rates, which are severely affected in the *mre11* null-type mutants (Ajimura *et al*., 1993; Johzuka and Ogawa, 1995; Nairz and Klein, 1997; Tsukamoto *et al*., 1997; Boulton and Jackson, 1998; Tsubouchi and Ogawa, 1998). In meiosis, meiotic DSBs can be formed, but no resection of DSBs occurs in *mre11D16A* as in the case of *mre11S* or *mre11-58* (Nairz and Klein, 1997; Tsubouchi and Ogawa, 1998). These results indicate that the nuclease domain is required for some types of DSB repair (i.e. repair of MMS-damaged DNA and meiotic DSBs) and telomere maintenance. It is demonstrated that the nuclease activities of Mre11 *per se* are not important for normal growth rate and suppression of interchromosomal recombination in mitosis, and DSB formation in meiosis, since no nuclease activity was detected in Mre11D16A protein. Mre11 is involved in both homologous recombination and NHEJ pathways possibly localizing at the gateway for both pathways. Preliminary results indicated that the *mre11D16A* mutant showed deficiency in target integration of yeast sequences into homologous chromosomal regions but was proficient in end-joining repair of linearized plasmid DNA (M.Furuse, Y.Nagase, T.Shibata and K.Ohta,

Table II. Effects of *MRE11* mutations on spore formation and spore viability

Mutant	No. of asci dissected	No. of viable spores					Spore viability	Spore formation
		4+	3+	2+	1+	0		
Wild-type (YMD302)	80	78	2	0	0	0	99%	99%
mre11Δnull (YMD1599)	80	0	0	0	0	80	<0.3%	49%
mre11D16A (YMD316)	80	0	0	0	0	80	<0.3%	11%
mre11ΔC49 (YMD325)	80	0	0	0	0	80	<0.3%	51%

Sporulation culture was as described in Materials and methods. For spore formation, we analyzed the population of the asci (>100) with >1 spores in all visible cells after 48 h.

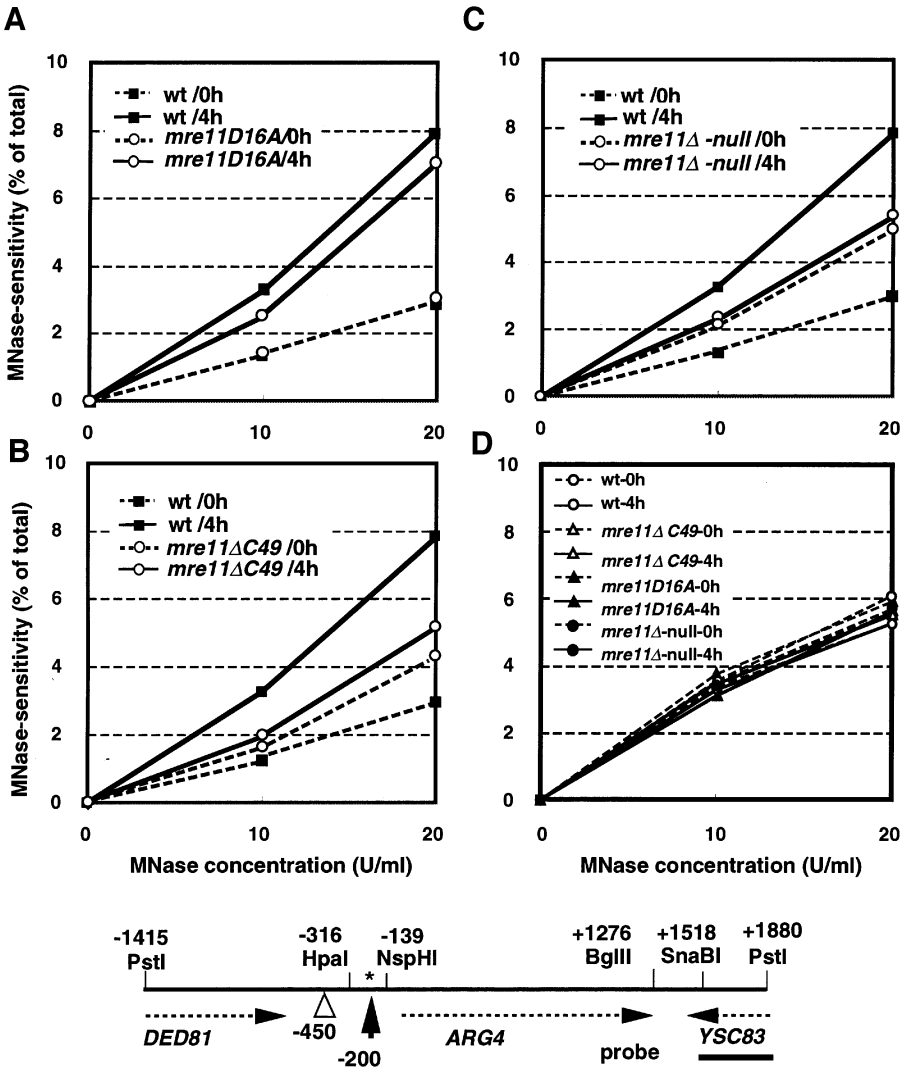

Fig. 9. Chromatin configuration at the *ARG4* DSB is aberrant in *mre11ΔC49* strain. Chromatin from diploid strains of YMD1599 (a *mre11* null mutant), YMD302 (wild-type), YMD316 (*mre11D16A*), and YMD325 (*mre11ΔC49*) was prepared from cells at 0 and 4 h after meiotic induction. Chromatin was further treated with 10 and 20 U/ml of MNase, and analyzed by an indirect end-labeling method as described (Ohta *et al*., 1994, 1998). MNase hypersensitivity (expressed as % relative to total band intensity) at the *ARG4* DSB site (at –200, shown by an arrow in the lower diagram) (**A**–**C**) and a non-DSB sensitive site (at –450) (**D**) in *mre11D16A* (A and D), *mre11ΔC49* (B and D) and *mre11Δ* null (C and D) is plotted as a function of MNase concentration. The mutant and wild-type cultures were analyzed in parallel on the same day. For comparison, all mutant data are indicated with wild-type data for the internal standard taken on the same day. Closed symbols, wild-type; open symbols, mutants. Dashed lines, 0 h (premeiosis); solid lines, 4 h (meiosis). Note that mutant effects were only detected at the DSB site but not at the control sensitive site and are not dependent on the concentration of MNase. The lower diagram indicates the positions for restriction sites, MNase hypersensitive sites (shown by a vertical arrow) and a control MNase sensitive site (an open arrowhead) for an internal standard. Coordinates are indicated respective to position +1, the first base of the *ARG4* coding region. An asterisk indicates the position of the meiotic DSBs. Horizontal broken arrows represent the orientation of the transcripts indicated. A horizontal thick bar shows the probe used in the present study.

unpublished observations). Therefore, it can be hypothesized that *mre11D16A* allele is deficient in some steps of homologous recombination pathways but proficient in NHEJ pathways both in mitosis and meiosis. This allele may provide an important clue to understanding the roles of Mre11 protein in the regulation of homologous recombination and NHEJ as well as its role in telomere maintenance and suppression of mitotic recombination.

The *mre11D16A* mutant showed deficiency in the processing of meiotic DSB ends. The same phenotype is found in *rad50S* and *mre11S* (*mre11-58*) mutants (Cao *et al*., 1990; Nairz and Klein, 1997; Tsubouchi and Ogawa, 1998). In these mutants, Spo11 protein is left attached covalently to DSB ends. These results suggest that the nuclease activities of Mre11 protein are involved in the end-processing of meiotic DSBs probably by removing Spo11 protein from the ends of DSBs. It is interesting to test if Mre11 can release the Spo11 *in vitro* from the Spo11–DNA complex isolated from meiotic cells of *rad50S* or *mre11S* strains. Otherwise, Mre11 exonuclease activity in yeast cells might be important for the resection of DSB ends to form ssDNA tails. However, it has 3′ to 5′ double-strand exonuclease activity *in vitro* as detected in human Mre11 protein (Paull and Gellert, 1998; Trujillo *et al*., 1998), which is opposite to the direction predicted from *in vivo* observation (Lee *et al*., 1988). One could speculate that an important cofactor for 5′ to 3′ exonuclease activity of Mre11 may be missing in *E.coli*-expressed Mre11

protein fraction, since the nuclease activity shows a strict Mn-dependence that is often seen in other nucleases without the essential cofactor. Alternatively, it is possible that long 3′ ssDNA tails might be generated by endo/exonuclease activity of Mre11 combined with unidentified helicase components in the recombination initiation complex as is the case for RecBCD in *E.coli* (Anderson and Kowalczykowski, 1997). On the other hand, we cannot exclude other possibilities for the deficiency in the processing of DSB ends. For example, a deficiency of Mre11D16A protein in the interaction of other proteins such as Rad50 could be an alternate reason for the lack of the end processing function.

Roles of the C-terminal dsDNA-binding domain in meiotic functions

The present results indicate that the C-terminal region of Mre11 is very important in meiotic functions of Mre11. The mutant *mre11ΔC49* was almost wild-type in mitosis, but showed severe deficiencies in meiosis. There was no induction of meiotic homologous recombination and no DSB formation in the *mre11ΔC49* strain, thereby spore formation and spore viability were reduced. Meiotic chromatin configuration at the *ARG4* DSB site was aberrant in the *mre11ΔC49* strain as observed in the *mre11* null mutant. Thus, the C-terminal domain of Mre11 protein is likely to play a pivotal role in the activation of homologous recombination in meiosis. These observations can be explained by indirect effects such as a deficiency of nuclear localization of Mre11ΔC49 protein or a meiosis-specific degradation of the Mre11Δ49 protein. However, the mitotic *mre11ΔC49* cells underwent repair of MMS-damaged DNA as efficiently as in the wild-type cells, indicating that Mre11ΔC49 protein can enter the nucleus. In addition, we could not detect any difference in the turnover between the Mre11ΔC49 and the wild-type Mre11 proteins in meiotic cells (data not shown). These results favor more direct effects of the *mre11ΔC49* mutation in meiotic recombination.

Biochemical analysis revealed a decrease in dsDNA-binding activity in the Mre11ΔC49 protein. Probably, the positively charged amino acids in the C-terminal region are involved in Mre11–dsDNA interaction. What is the significance of dsDNA binding of Mre11 through the C-terminal region? DSB sites in *S.cerevisiae* cells are always found in nucleosome-free open chromatin regions (Ohta *et al*., 1994; Wu and Lichten, 1994; Fan and Petes, 1996; Keeney and Kleckner, 1996). Therefore, in these sites, DNA should be exposed at least partially. Such exposed DNA might be a preferential target of dsDNA binding of Mre11 protein. In meiosis, Mre11 protein might interact with the exposed DNA in DSB sites through its C-terminal domain as a component of the 'pre-DSB complex' interacting with other meiosis-specific factors required for DSB formation such as Rec104, Spo11 and Mer2 protein (Klapholz and Esposito, 1982; Engebrecht *et al*., 1991; Malone *et al*., 1991; Cool and Malone, 1992; Rockmill *et al*., 1995; Keeney *et al*., 1997). This notion seems consistent with our previous and present observations. We previously reported that there was a phase transition in chromatin configuration at DSB sites during meiosis that is dependent on the function of Mre11 and Mre2 which is involved in meiotic activation and meiosis-specific splicing of *MER2* gene (Ohta *et al*., 1994, 1998; Nakagawa and Ogawa, 1997). In addition, present results indicate that the C-terminal region of Mre11 is essential in the meiotic transition of chromatin configuration at DSB sites. It would be interesting to examine effects of expression of the C-terminal region in *mre11* null mutant on meiotic phenotypes and to look at the interaction of the C-terminal domain of Mre11 protein with the meiosis-specific proteins.

Conserved roles of Mre11 in higher eukaryotes?

Recent studies have suggested that Mre11 is well conserved in other eukaryotic species (Petrini *et al*., 1995; Sharples and Leach, 1995; Tavassoli *et al*., 1995; Paull and Gellert, 1998). Amino acid sequences of Mre11 proteins in various organisms are quite similar, especially in the phosphoesterase domains. In addition, overall domain structure is also preserved. In all cases, Mre11 consists of the N-terminal SbcD-like phosphoesterase domain and clustering of basic or acidic amino acids in the C-terminal region (see Figure 1). Such conservation is not limited in the primary structure of Mre11. Complex formation of Mre11 with Rad50 and Xrs2 can be detected not only in yeast but also in human cells (Johzuka and Ogawa, 1995; Dolganov *et al*., 1996; Carney *et al*., 1998). Probably, Mre11 proteins in higher eukaryotes may also be involved in DNA-damage repair and meiotic recombination as observed in yeast cells. Thus, to test the generality, it is interesting to introduce mutations at important conserved amino acids in Mre11. The Asp16 is conserved in Mre11 proteins in some model organisms including *Schizosaccharomyces pombe* (Tavassoli *et al*., 1995) and mouse (DDBJ/EMBL/GenBank accession No. U58987). By introducing a mutation at this amino acid in Mre11 of higher eukaryotes, it may be possible to detect DSB formation in meiosis of eukaryotes other than *S.cerevisiae*.

Materials and methods

Strains, cultures and sporulation

All media used here are as described (Sherman *et al*., 1979). All yeast strains listed in Table III are with the SK1 background. Premeiotic and sporulation cultures were as described previously (Ohta *et al*., 1994, 1998). Progression of meiosis was monitored and confirmed by nuclei staining with 4′,6′-diamidino-2-phenylindole (Ohta *et al*., 1994).

Isolation of MRE11 gene and introduction of mutations

The *MRE11* gene was isolated from a genomic library of the DBY939 strain from Carlson and Botstein (1982) by colony hybridization using a DNA fragment for the *MRE11* coding sequence, which was obtained by PCR. The site-directed mutagenesis at Asp16 (*mre11D16A*) was introduced by PCR according to the oligonucleotide-directed dual amber method (Hashimoto-Gotoh *et al*., 1995). The deletion of the C-terminal domain (*mre11ΔC49*) was prepared by converting the Ser644 (AGT) to a termination codon (TAG). Plasmids for *E.coli* expression were constructed by the insertion of the wild-type *MRE11*, *mre11D16A*, and *mre11ΔC49* sequences into pRSET-B plasmid to introduce a $(His)_6$-tag in the N-termini. We confirmed DNA sequences of the insertions in all three constructs. Yeast gene replacement was carried out by homologous recombination after transforming linearized DNA fragment of the wild-type *MRE11*, *mre11D16A*, and *mre11ΔC49* sequences flanked with the *URA3* gene in the 3′ regions. Positive clones (Ura^+ colonies) were selected on Ura^- minimum medium plates and further confirmed by Southern hybridization of the genomic DNA cleaved by appropriate restriction enzymes.

Table III. Strains used in this study

Diploid	Haploid	Genotypes	Source
MJL1720	S799	*MATa ura3 lys2 ho::LYS2 leu2Δ arg4-bgl cyh2-z*	M.Lichten
	S800	*MATα ura3 lys2 ho::LYS2 leu2Δ arg4-nsp cyh2-z*	M.Lichten
YMD1599	YMD799	*MATa ura3 lys2 ho::LYS2 leu2Δ arg4-bgl cyh2-z mre11Δ(acc-aor51)::URA3*	this study
	YMD800	*MATα ura3 lys2 ho::LYS2 leu2Δ arg4-nsp cyh2-z mre11Δ(acc-aor51)::URA3*	this study
YMD302	YMW7-2B	*MATa ura3 lys2 ho::LYS2 leu2Δ arg4-bgl cyh2-z MRE11::URA3*	this study
	YMW8-2B	*MATα ura3 lys2 ho::LYS2 leu2Δ arg4-nsp cyh2-z MRE11::URA3*	this study
YMD316	YMM7-3A	*MATa ura3 lys2 ho::LYS2 leu2Δ arg4-bgl cyh2-z mre11D16A::URA3*	this study
	YMM8-3C	*MATα ura3 lys2 ho::LYS2 leu2Δ arg4-nsp cyh2-z mre11D16A::URA3*	this study
YMD325	YMM7-1B	*MATa ura3 lys2 ho::LYS2 leu2Δ arg4-bgl cyh2-z mre11ΔC49::URA3*	this study
	YMM8-1B	*MATα ura3 lys2 ho::LYS2 leu2Δ arg4-nsp cyh2-z mre11ΔC49::URA3*	this study
MJL1699	S789	*MATa ura3 lys2 ho::LYS2 leu2Δ arg4-bgl* rad50-KI81::URA3	M.Lichten
	S793	*MATα ura3 lys2 ho::LYS2 leu2Δ arg4-nsp rad50-KI81::URA3*	M.Lichten

All strains are with the SK1 background.

Purification of (His)$_6$-tagged Mre11 proteins

Proteins were expressed in BL21(DE3) *E.coli* strain carrying a plasmid pLys at 18°C for 12 h in the presence of 0.4 mM of isopropyl-β-D-thiogalactopyranoside. Cells (2–5 g) were broken by freeze–thawing and sonication in 6 ml/g cells of an ice-cold binding buffer containing 10 mM Tris–HCl pH 8.0, 5 mM imidazole, 500 mM NaCl, 10% glycerol and 0.05% Triton X-100, supplemented with 1 mM of Pefablock SC [4-(2-aminoethyl)-benzenesulfonyl fluoride hydrochloride, Boehringer Mannheim] and a protease inhibitor cocktail (Complete EDTA-free, Boehringer Mannheim). Broken cells were centrifuged at 12 000 *g* for 1 h at 4°C. The supernatant was then applied to TALON Co^{2+}-affinity column chromatography (1.5 ml bed volume/g cells, Clontech). Mre11 was fractionated in the binding buffer by a linear gradient of 5–100 mM imidazole according to the manufacturer's instructions. Typical yield in the pooled TALON fraction was 3.5 mg of $(His)_6$-Mre11/g cells. To confirm that this protein is Mre11 protein, we raised an antibody to the TALON-purified Mre11 protein and analyzed the antigen in cell extracts of the wild-type and a *mre11* null mutant by immunoblotting. In this experiment, we detected an ~80 kDa-single band in the wild-type extract that was not detected in the null mutant, indicating that this protein is actually Mre11.

The TALON-purified fraction (7–20 mg of proteins) was diluted 10 times in a H20 buffer (20 mM HEPES pH 7.4, 10% glycerol, 0.5 mM $MgCl_2$) and further applied to a dsDNA–cellulose column (Sigma, 3 mg calf thymus DNA/g solid, 3 ml bed volume) or a heparin–Sepharose column (7 ml of bed volume, Seikagaku-kogyo) pre-equilibrated with H20 buffer containing 50 mM NaCl. Mre11 protein was eluted by a linear gradient of 50–1000 mM NaCl. Mre11 was recovered around the concentration of 300–400 mM NaCl in the dsDNA–cellulose column and at 500 mM NaCl in the heparin–Sepharose column. TALON-purified Mre11ΔC49 protein was diluted 10 times in a H20 buffer, and was applied to Q–Sepharose FF column (7 ml of bed volume, Amersham Pharmacia). Mre11ΔC49 protein was eluted at 300 mM NaCl from a linear gradient of 50–1000 mM NaCl. The purity and the yield at these steps were >98% and 1.2–1.8 mg/g cells. Mre11 proteins (2–5 mg) after heparin–Sepharose, dsDNA–cellulose, or Q–Sepharose FF columns were further fractionated through phenyl–Sepharose CL-4B (5 ml bed volume, Amersham Pharmacia) using a step-wise elution by H20 buffer containing 0, 20 and 40% ethylene glycol and 50 mM NaCl. Mre11 was eluted at 40% ethylene glycol. The purity and the yield at this step were nearly homogenous and 0.6–0.9 mg/g cells.

Gel filtration of Mre11 proteins

Heparin-purified or Q–Sepharose purified Mre11 proteins (200 µl, 50–100 µg) were fractionated through a high performance gel-filtration column (Superose 12 HR with an exclusion limit of ~2×10^6 M_r, Amersham Pharmacia) pre-equilibrated in the H20 buffer containing 0.5 M NaCl at a flow rate of 0.5 ml/min and a pressure of 2 M Pascal. The peak of Mre11 was detected in-line UV monitor and SDS–polyacrylamide gel electrophoresis (Laemmli, 1970). Molecular weight standards [catalase, aldolase, bovine serum albumin (BSA), ovalbumin, chymotrypsin, RNase A, tryptophan] were also applied to the column to generate a standard curve.

Band-shift assay

Mre11 proteins (0–4 µg, 0–50 pmol) of phenyl–Sepharose CL4B or heparin–Sepharose fractions were incubated with 50 ng of pUC119 form III DNA (154 pmol phosphate, final 7.7 µM phosphate) in 20 µl of reaction mixture containing 20 mM HEPES (pH 7.4), 150 mM NaCl, 0 or 5 mM $MgCl_2$, and 0.2 mg/ml BSA at 30°C for 10 min. The protein–DNA complex was directly separated in a 0.8% agarose gel and stained with ethidium bromide.

Oligonucleotide substrates (listed below, 5 nmol phosphate, final 250 µM phosphate, 170 pmol molecules) were incubated with (0–10 µg, 0–125 pmol) of heparin-purified Mre11 proteins in a 20 µl of reaction mixture containing 10 mM Tris–HCl (pH 7.5), 10 mM $MgCl_2$, 1 mM dithiothreitol (DTT) and 0.2 mg/ml BSA at 30°C for 30 min. The protein–DNA complex was directly separated in a 4% non-denaturing acrylamide gel, stained with ethidium bromide, and analyzed by FM-BIO II fluorescence image analyzer (Hitachi). Complex formation rates are ratios (%) of fluorescence in the shifted band to the unbound origin.

Radioactive oligonucleotides (Aarg4 and T14, see below) were prepared by labeling with ^{32}P at the 5′ end using Megalabel 5′-labeling kit (Takara). Non-labeled oligonucleotide substrates (5 nmol phosphate, final 250 µM phosphate, 170 pmol molecules) were added to 20 fmol molecules of ^{32}P-labeled oligonucleotides, and then incubated with (0–4 µg, 0–50 pmol) of heparin-purified Mre11 proteins in 10 µl of a reaction mixture containing 10 mM Tris–HCl (pH 7.5), 10 mM $MgCl_2$, 1 mM DTT and 0.2 mg/ml BSA at 30°C for 30 min. Anti-Mre11ΔC49 protein used in a supershift experiment was raised in rabbits and specific antibody was affinity purified with Mre11ΔC49 protein according to the method of Towbin *et al*. (1979). The protein–DNA complex was directly separated in a 4% non-denaturing acrylamide gel, and visualized and quantified by BAS2000 image analyzer. Complex formation rates are ratios (%) of radioactivity in the shifted band to the unbound origin.

Assay of nuclease activities

Linearized plasmid DNA was prepared by treating pUC119 DNA with *Eco*RI followed by phenol extraction and ethanol precipitation. Mre11 proteins (0–8 µg, 0–100 pmol) in heparin–Sepharose, Q–Sepharose FF, or dsDNA–cellulose fractions were incubated with M13mp18 ssDNA (200 ng, 308 pmol phosphate, final 15.4 µM phosphate), linearized

pUC119 DNA (50 ng, 154 pmol phosphate, final 7.7 μM phosphate), or ds-oligonucleotides (2.35 nmol phosphate, final 118 μM phosphate, 160 pmol DNA ends) in 20 μl of a standard reaction mixture (20 mM HEPES pH 7.4, 150 mM NaCl, 5 mM $MnCl_2$, 0.1 mM DTT, 0.2 mg/ml BSA) was incubated at 30°C or 37°C for 1 h. The radioactive pUC119 *Eco*RI fragment was prepared by labeling with ^{32}P at the 5′ end as described above. We incubated 5 ng (15.4 pmol phosphate, final 0.77 μM phosphate) of 5′ ^{32}P-labeled pUC119 *Eco*RI fragment with 3 μg (37.5 pmol) of Mre11 protein for an indicated time. The reaction was terminated by adding 2 μl of a stop solution (100 mM EDTA and 10% SDS) to the mixture. DNA was extracted by phenol/$CHCl_3$/isoamylalchol, separated in agarose (0.8%, for M13 and pUC DNA) and polyacrylamide (20%, for oligonucleotides) gels. Bands were detected by staining with ethidium bromide or autoradiography.

Analysis of telomere length and DSB detection, return-to-growth experiment

DNA for DSB detection and telomere analysis was prepared from the cells harvested at indicated times following the start of the meiotic culture according to the method of Cao *et al*. (1990) and Ohta *et al*. (1994), respectively. DNA was digested with indicated restriction endonucleases and analyzed by Southern hybridization as described (Wu and Lichten, 1994; Boulton and Jackson, 1998) according to the method of Church and Gilbert (1984). For telomere detection, genomic DNA (2 μg) was digested with *Xho*I, separated in 0.8% agarose gel, transferred to Hybond N^+ (Amersham) using a method of alkaline transfer and hybridized with a 5′ ^{32}P-labeled poly$(GT)_{20}$ oligonucleotide. For detection of DSB in *YCR48w/YCR47c*, genomic DNA (2 μg) was digested with *Bgl*II, separated in 0.7% agarose gel, transferred to Hybond N^+, and hybridized with a ^{32}P-labeled *Hin*dIII–*Hin*dIII 0.9 kb DNA fragment. Return-to-growth experiment was performed as described elsewhere (Ohta *et al*., 1994).

Analysis of chromatin structure

Chromatin was prepared from the cells cultured for 0 and 4 h in the sporulation medium, and then treated with MNase as describe (Ohta *et al*., 1994, 1998). DNA was digested with *Pst*I, separated in agarose gels, transferred to Hybond N^+ (Amersham). Radioactive probes were prepared by random priming of the *Pst*I–*Sna*B I DNA fragments from the pUC119/*ARG4*-Pst plasmid (Ohta *et al*., 1994). Hybridizations of membranes were carried out according to the method of Church and Gilbert (1984). Radioactivity was visualized by a BAS2000 image analyzer (Fuji) and quantified by a Bioimage intelligent quantifyer as described previously (Ohta *et al*., 1994). Radioactivity of the *ARG4* DSB site (–200 bp from the first A of the initiation codon of the Arg4 coding sequence) and the control site (–450 bp) was expressed % relative to the total radioactivities.

Oligonucleotide for DNA-binding assays

P105-T: 5′-GATCCTCGTCACTTCCAATATGAATGCG-3′ (28mer)
P105-B: 5′-GATCCGCATTCATATTGGAAGTGACGAG-3′ (28mer)
Aarg4: 5′-AATCATGATTAGTAGATGAATGACTCACTT-3′ (30mer)
BantiA: 5′-AAGTGAGTCATTCATCTACTAATCATGATT-3′ (30mer)
C2nt3: 5′-AAGTGAGTCATTCATCTACTAATCATGA-3′ (28mer)
D7nt3: 5′-AAGTGAGTCATTCATCTACTAAT-3′ (23mer)
E15nt3: 5′-AAGTGAGTCATTCAT-3′ (15mer)
F2nt5: 5′-GTGAGTCATTCATCTACTAATCATGATT-3′ (28mer)
G7nt5: 5′-TCATTCATCTACTAATCATGATT-3′ (23mer)
H15nt5: 5′-CTACTAATCATGATT-3′ (15mer)
I3ntmis: 5′-AAGTGAGTCATTCAGAGACTAATCATGATT-3′ (30mer)
J6ntmis: 5′-AAGTGAGTCATTACGAGCCTAATCATGATT-3′ (30mer)
K5over7: 5′-TCCCGAAAATCATGATTAGTAGATGAATGA-3′ (30mer)
L3over7: 5′-TCATTCATCTACTAATCATGATTTTCGGGA-3′ (30mer)
T14: 5′-TTTTTTTTTTTTTT-3′

A double-stranded substrate with cohesive ends was composed of P105-T and P105-B. Substrates with blunt ends, 3′-2 nt, 7 nt, 15 nt overhangs were composed of Aarg4 and BantiA, Aarg4 and C2nt3, Aarg4 and D7nt3, Aarg4 and E15nt3, respectively. Substrates with 5′-2 nt, 7 nt, 15 nt overhangs were composed of Aarg4 and F2nt5, Aarg4 and G7nt5, Aarg4 and H15nt5, respectively. Substrates with 5′-7 nt and 3′-7 nt overhangs at both ends were composed of K5over7 and BantiA, and Aarg4 and L3over7, respectively. Bubble-mismatched substrates were composed of Aarg4 and I3ntmis, or Aarg4 and I6ntmis, respectively. Annealing was performed at 30°C for 30 min.

Oligonucleotides for PCR

M11F: 5′-CGACCATGGACTATCCTGATCCAG-3′
(Initiation codon is underlined. *Nco*I site is created.)
M11RΔC49: 5′-CGGTCGACCATAACTAGGCGTCCTCTTC-3′
(Termination codon is underlined.)
M11FD16A: 5′-GATTTTAATTACTACAGCTAATCATGTGGG-3′

Acknowledgements

We thank E.Kobayashi for her assistance in the biochemical analyzes of Mre11 proteins. We are also grateful to A.Nicolas (Institut Curie, France), H.Ogawa (Osaka University, Japan) and K.Mizuno (this laboratory) for stimulating discussions on the results, M.Lichten (National Institute of Health, USA) for the kind gift of strains S799 and S800, and J.Sassoon (this laboratory) for proofreading the manuscript. This work was supported by a research grant from the Human Frontier Science Program (RG493/95), a grant for the 'Biodesign Research Program' from RIKEN, CREST of JST (Japan Science and Technology), and grants from the Ministry of Education, Science and Culture, Japan.

References

Ajimura,M., Leem,S.H. and Ogawa,H. (1993) Identification of new genes required for meiotic recombination in *Saccharomyces cerevisiae*. *Genetics*, **133**, 51–66.

Alani,E., Padmore,R. and Kleckner,N. (1990) Analysis of wild-type and *rad50* mutations of yeast suggests an intimate relationship between meiotic chromosome synapsis and recombination. *Cell*, **61**, 419–436.

Anderson,D.G. and Kowalczykowski,S.C. (1997) The recombination hot spot chi is a regulatory element that switches the polarity of DNA degradation by the RecBCD enzyme. *Genes Dev.*, **11**, 571–581.

Bergerat,A., de Massy,B., Gadelle,D., Varoutas,P.C., Nicolas,A. and Forterre,P. (1997) An atypical topoisomerase II from *Archaea* with implications for meiotic recombination. *Nature*, **386**, 414–417.

Boulton,S.J. and Jackson,S.P. (1996) *Saccharomyces cerevisiae* Ku70 potentiates illegitimate DNA double-strand break repair and serves as a barrier to error-prone DNA repair pathways. *EMBO J.*, **15**, 5093–5103.

Boulton,S.J. and Jackson,S.P. (1998) Components of the Ku-dependent non-homologous end-joining pathway are involved in telomeric length maintenance and telomeric silencing. *EMBO J.*, **17**, 1819–1828.

Cao,L., Alani,E. and Kleckner,N. (1990) A pathway for generation and processing of double-strand breaks during meiotic recombination in *S.cerevisiae*. *Cell*, **61**, 1089–1101.

Carlson,M. and Botstein,D. (1982) Two differentially regulated mRNAs with different 5′ ends encode secreted with intracellular forms of yeast invertase. *Cell*, **28**, 145–154.

Carney,J.P., Maser,R.S., Olivares,H., Davis,E.M., Le Beau,M., Yates, J.R. III, Hays,L., Morgan,W.F. and Petrini,J.H. (1998) The hMre11/hRad50 protein complex and Nijmegen breakage syndrome: linkage of double-strand break repair to the cellular DNA damage response. *Cell*, **93**, 477–486.

Church,G.M. and Gilbert,W. (1984) Genomic sequencing. *Proc. Natl Acad. Sci. USA*, **81**, 1991–1995.

Cohen,P.T., Collins,J.F., Coulson,A.F., Berndt,N. and da Cruz e Silva,O.B. (1988) Segments of bacteriophage lambda (orf 221) and phi 80 are homologous to genes coding for mammalian protein phosphatases. *Gene*, **69**, 131–134.

Connelly,J.C. and Leach,D.R. (1996) The sbcC and sbcD genes of *Escherichia coli* encode a nuclease involved in palindrome inviability and genetic recombination. *Genes Cells*, **1**, 285–291.

Cool,M. and Malone,R.E. (1992) Molecular and genetic analysis of the yeast early meiotic recombination genes *REC102* and *REC107*/*MER2*. *Mol. Cell. Biol.*, **12**, 1248–1256.

Dolganov,G.M., Maser,R.S., Novikov,A., Tosto,L., Chong,S., Bressan,D.A. and Petrini,J.H. (1996) Human Rad50 is physically associated with human Mre11: identification of a conserved multiprotein complex implicated in recombinational DNA repair. *Mol. Cell. Biol.*, **16**, 4832–4841.

Engebrecht,J.A., Voelkel-Meiman,K. and Roeder,G.S. (1991) Meiosis-specific RNA splicing in yeast. *Cell*, **66**, 1257–1268.

Fan,Q.Q. and Petes,T.D. (1996) Relationship between nuclease-hypersensitive sites and meiotic recombination hot spot activity at the *HIS4* locus of *Saccharomyces cerevisiae*. *Mol. Cell. Biol*., **16**, 2037–2043.

Farnet,C., Padmore,R., Cao,L., Raymond,W., Alani,E. and Kleckner,N. (1988) The *RAD50* gene of *S.cerevisiae*. In Frieberg,E. and Handbalt,P. (eds), *Mechanisms and Consequences of DNA Damage Processing*. (UCLA Symposia on Molecular and Cellular Biology) vol. **83**, Alan R.Liss, Inc., New York pp. 1–15.

Game,J.C. and Motimer,R.K. (1974) A genetic study of X-ray sensitive mutants in yeast. *Mutat. Res*., **24**, 281–292.

Griffith,J.P. *et al*. (1995) X-ray structure of calcineurin inhibited by the immunophilin-immunosuppressant FKBP12–FK506 complex. *Cell*, **82**, 507–22.

Guerini,D. and Klee,C.B. (1989) Cloning of human calcineurin A: evidence for two isozymes and identification of a polyproline structural domain. *Proc. Natl Acad. Sci. USA*, **86**, 9183–9187.

Haber,J.E. (1995) *In vivo* biochemistry: physical monitoring of recombination induced by site-specific endonucleases. *Bioessays*, **17**, 609–620.

Hashimoto-Gotoh,T., Mizuno,T., Ogasahara,Y. and Nakagawa,M. (1995) An oligodeoxyribonucleotide-directed dual amber method for site-directed mutagenesis. *Gene*, **152**, 271–275.

Ivanov,E.L., Korolev,V.G. and Fabre,F. (1992) *XRS2*, a DNA repair gene of *Saccharomyces cerevisiae*, is needed for meiotic recombination. *Genetics*, **132**, 651–664.

Johzuka,K. and Ogawa,H. (1995) Interaction of Mre11 and Rad50: two proteins required for DNA repair and meiosis-specific double-strand break formation in *Saccharomyces cerevisiae*. *Genetics*, **139**, 1521–1532.

Keeney,S. and Kleckner,N. (1996) Communication between homologous chromosomes: genetic alterations at a nuclease-hypersensitive site can alter mitotic chromatin structure at that site both *in cis* and *in trans*. *Genes Cells*, **1**, 475–490.

Keeney,S., Giroux,C.N. and Kleckner,N. (1997) Meiosis-specific DNA double-strand breaks are catalyzed by Spo11, a member of a widely conserved protein family. *Cell*, **88**, 375–384.

Kironmai,K.M. and Muniyappa,K. (1997) Alteration of telomeric sequences and senescence caused by mutations in RAD50 of *Saccharomyces cerevisiae*. *Genes Cells*, **2**, 443–455.

Kissinger,C.R. *et al*. (1995) Crystal structures of human calcineurin and the human FKBP12–FK506–calcineurin complex. *Nature*, **378**, 641–644.

Klapholz,S. and Esposito,R.E. (1982) A new mapping method employing a meiotic rec$^-$ mutant of yeast. *Genetics*, **100**, 387–412.

Kon,N., Krawchuk,M.D., Warren,B.G., Smith,G.R. and Wahls,W.P. (1997) Transcription factor Mts1/Mts2 (Atf1/Pcr1, Gad7/Pcr1) activates the M26 meiotic recombination hotspot in *Schizosaccharomyces pombe*. *Proc. Natl Acad. Sci. USA*, **94**, 13765–13770.

Kramer,K.M., Brock,J.A., Bloom,K., Moore,J.K. and Haber,J.E. (1994) Two different types of double-strand breaks in *Saccharomyces cerevisiae* are repaired by similar RAD52-independent, nonhomologous recombination events. *Mol. Cell. Biol*., **14**, 1293–1301.

Laemmli,U.K. (1970) Cleavage of structural proteins during the assembly of the head of bacteriophage T4. *Nature*, **227**, 680–685.

Leach,D.R., Lloyd,R.G. and Coulson,A.F. (1992) The SbcCD protein of *Escherichia coli* is related to two putative nucleases in the UvrA superfamily of nucleotide-binding proteins. *Genetica*, **87**, 95–100.

Lee,S.E., Moore,J.K., Holmes,A., Umezu,K., Kolodner,R.D. and Haber,J.E. (1998) *Saccharomyces* Ku70, Mre11/Rad50 and RPA proteins regulate adaptation to G2/M arrest after DNA damage. *Cell*, **94**, 399–409.

Loidl,J., Klein,F. and Scherthan,H. (1994) Homologous pairing is reduced but not abolished in asynaptic mutants of yeast. *J. Cell Biol*., **125**, 1191–1200.

Malone,R.E., Bullard,S., Hermiston,M., Rieger,R., Cool,M. and Galbraith,A. (1991) Isolation of mutants defective in early steps of meiotic recombination in the yeast *Saccharomyces cerevisiae*. *Genetics*, **128**, 79–88.

Matsuura,S. *et al*. (1998) Positional cloning of the gene for Nijmegen breakage syndrome. *Nature Genet.*, **19**, 179–181.

Mezard,C. and Nicolas,A. (1994) Homologous, homeologous and illegitimate repair of double-strand breaks during transformation of a wild-type strain and a *rad52* mutant strain of *Saccharomyces cerevisiae*. *Mol. Cell. Biol*., **14**, 1278–1292.

Milne,G.T., Jin,S., Shannon,K.B. and Weaver,D.T. (1996) Mutations in two Ku homologs define a DNA end-joining repair pathway in *Saccharomyces cerevisiae*. *Mol. Cell. Biol*., **16**, 4189–4198.

Moore,J.K. and Haber,J.E. (1996) Cell cycle and genetic requirements of two pathways of nonhomologous end-joining repair of double-strand breaks in *Saccharomyces cerevisiae*. *Mol. Cell. Biol*., **16**, 2164–2173.

Nairz,K. and Klein,F. (1997) *mre11S*-a yeast mutation that blocks double-strand-break processing and permits nonhomologous synapsis in meiosis. *Genes Dev.*, **11**, 2272–2290.

Nakagawa,T. and Ogawa,H. (1997) Involvement of the *MRE2* gene of yeast in formation of meiosis-specific double-strand breaks and crossover recombination through RNA splicing. *Genes Cells*, **2**, 65–79.

Nugent,C.I., Bosco,G., Ross,L.O., Evans,S.K., Salinger,A.P., Moore,J.K., Haber,J.E. and Lundblad,V. (1998) Telomere maintenance is dependent on activities required for end repair of double-strand breaks. *Curr. Biol*., **8**, 657–660.

Ogawa,H., Johzuka,K., Nakagawa,T., Leem,S.H. and Hagihara,A.H. (1995) Functions of the yeast meiotic recombination genes, *MRE11* and *MRE2*. *Adv. Biophys*., **31**, 67–76.

Ohta,K., Shibata,T. and Nicolas,A. (1994) Changes in chromatin structure at recombination initiation sites during yeast meiosis. *EMBO J*., **13**, 5754–5763.

Ohta,K., Nicolas,A., Furuse,M., Nabetani,A., Ogawa,H. and Shibata,T. (1998) Mutations in the *MRE11*, *RAD50*, *XRS2* and *MRE2* genes alter chromatin configuration at meiotic DNA double-stranded break sites in premeiotic and meiotic cells. *Proc. Natl Acad. Sci. USA*, **95**, 646–651.

Paull,T.T. and Gellert,M. (1998) The 3′ to 5′ exonuclease activity of Mre11 facilitates repair of DNA double-strand breaks. *Mol. Cell*, **1**, 969–979.

Petrini,J.H., Walsh,M.E., DiMare,C., Chen,X.N., Korenberg,J.R. and Weaver,D.T. (1995) Isolation and characterization of the human *MRE11* homologue. *Genomics*, **29**, 80–86.

Rockmill,B., Engebrecht,J.A., Scherthan,H., Loidl,J. and Roeder,G.S. (1995) The yeast *MER2* gene is required for chromosome synapsis and the initiation of meiotic recombination. *Genetics*, **141**, 49–59.

Sharples,G.J. and Leach,D.R. (1995) Structural and functional similarities between the SbcCD proteins of *Escherichia coli* and the *RAD50* and *MRE11* (*RAD32*) recombination and repair proteins of yeast. *Mol. Microbiol*., **17**, 1215–1217.

Sherman,F., Fink,G.R. and Laurence,C. (1979) *Methods in Yeast Genetics*. Cold Spring Harbor Laboratory Press, Cold Spring Harbor, NY.

Shinohara,A. and Ogawa,T. (1995) Homologous recombination and the roles of double-strand breaks. *Trends Biochem. Sci*., **20**, 387–391.

Tavassoli,M., Shayeghi,M., Nasim,A. and Watts,F.Z. (1995) Cloning and characterisation of the *Schizosaccharomyces pombe rad32* gene: a gene required for repair of double strand breaks and recombination. *Nucleic Acids Res*., **23**, 383–388.

Towbin,H., Staehelin,T. and Gordon,J. (1979) Electrophoretic transfer of proteins from polyacrylamide gels to nitrocellulose sheets: procedure and some applications. *Proc. Natl Acad. Sci. USA*, **76**, 4350–4354.

Trujillo,K.M., Yuan,S.S.F., Lee,E.Y.H.P. and Sung,P. (1998) Nuclease activities in a complex of human recombination and DNA repair factors rad50, mre11 and p95. *J. Biol. Chem*., **273**, 21447–21450.

Tsubouchi,H. and Ogawa,H. (1998) A novel *mre11* mutation impairs processing of double-strand breaks of DNA during both mitosis and meiosis. *Mol. Cell. Biol*., **18**, 260–268.

Tsukamoto,Y. and Ikeda,H. (1998) Double-strand break repair mediated by DNA end-joining. *Genes Cells*, **3**, 135–144.

Tsukamoto,Y., Kato,J. and Ikeda,H. (1996) Hdf1, a yeast Ku-protein homologue, is involved in illegitimate recombination, but not in homologous recombination. *Nucleic Acids Res*., **24**, 2067–2072.

Tsukamoto,Y., Kato,J. and Ikeda,H. (1997) Budding yeast Rad50, Mre11, Xrs2 and Hdf1, but not Rad52, are involved in the formation of deletions on a dicentric plasmid. *Mol. Gen. Genet*., **255**, 543–547.

Varon,R. *et al*. (1998) Nibrin, a novel DNA double-strand break repair protein, is mutated in Nijmegen breakage syndrome. *Cell*, **93**, 467–476.

Weiner,B.M. and Kleckner,N. (1994) Chromosome pairing via multiple interstitial interactions before and during meiosis in yeast. *Cell*, **77**, 977–991.

Wu,T.-C. and Lichten,M. (1994) Meiosis-induced double-strand break sites determined by yeast chromatin structure. *Science*, **263**, 515–518.

Zhuo,S., Clemens,J.C., Stone,R.L. and Dixon,J.E. (1994) Mutational analysis of a Ser/Thr phosphatase: identification of residues important in phosphoesterase substrate binding and catalysis. *J. Biol. Chem*., **269**, 26234–26238.

Received July 27, 1998; revised September 8, 1998; accepted September 10, 1998